Maximizing spike train coherence or incoherence in the leaky integrate-and-fire model

Benjamin Lindner and Lutz Schimansky-Geier

Institute of Physics, Humboldt-University at Berlin, Invalidenstrasse 110, D-10115 Berlin, Germany

André Longtin

Department of Physics, University of Ottawa, 150 Louis Pasteur, Ottawa, Canada KIN 6N5

We study noise-induced resonance effects in the leaky integrate-and-fire neuron model with absolute refractory period, driven by a Gaussian white noise. It is demonstrated that a finite noise level may either maximize or minimize the regularity of the spike train. We also partition the parameter space into regimes where either or both of these effects occur. It is shown that the coherence minimization at moderate noise results in a flat spectral response with respect to periodic stimulation in contrast to sharp resonances that are observed for both small and large noise intensities.

Coherence resonance (CR) is the effect of noise-enhanced regularity of an excitable system's output. It has been found in a number of theoretical models [1–4] and experimental systems [5–8]. The systems discussed so far are multidimensional for which only a few analytical attempts have been made [9,10]. This may lead to the conjecture that the effect cannot be found in one-dimensional systems as is sometimes asserted in the literature [11]. In contrast, it was shown numerically by Pakdaman *et al*. [12] that coherence resonance can be observed in a one-dimensional model with a threshold condition, namely, the leaky integrate-and-fire (LIF) model that is the work horse of many theoretical studies in neurobiology. Here we employ exact expressions for the most common measures of coherence resonance to study the effect in the LIF model. Moreover, by means of these results we will demonstrate that the inverse effect can appear, too. If an absolute refractory period is included, a most irregular spiking can be obtained if the noise intensity is at a finite value. We further show that this effect manifests itself at different noise intensities depending on which statistic is used to measure coherence. Both coherence resonance and incoherence maximization may indicate biologically relevant functionalities as we will discuss at the end of this work.

The LIF model describes the dynamics of the voltage across the nerve membrane between excitations by an Ornstein-Uhlenbeck process

$$\dot{v} = -v + \mu + \sqrt{2D}\,\xi(t) \qquad (1)$$

where we have set the membrane time constant to 1 (variable and parameters are nondimensional). The parameter D stands for the intensity of the white Gaussian noise while μ denotes the base current which we consider as a parameter rather than an input. A strong nonlinearity of the model is introduced by a threshold condition: whenever the voltage reaches v_T, a spike is fired; we set $v_T = 1$ throughout our study. After excitation, the neuron is for time τ in an absolute refractory state followed by a reset to $v_R = 0$. The output spike train can be expressed by

$$x(t) = \sum_{t_i \in \mathcal{T}} \delta(t - t_i) \qquad (2)$$

where $\mathcal{T}$ is the set of spiking times generated by the model. The spike count in time window $(0,t)$ is the integral of the output

$$n(t) = \int_0^t dt'\, x(t'). \qquad (3)$$

In Fig. 1, the model is illustrated for the excitable case also referred to as the *noise-activated firing (subthreshold) regime*: the resting state of the deterministic system $v^* = \mu$ (for which $\dot{v} = 0$ at $D = 0$) is smaller than the threshold (i.e., $v^* = \mu < v_T$). For this case the neuron fires only in the presence of noise. Furthermore, there are three time scales involved in the process: first, the relaxation time for passage from the reset point to the resting value, second, the escape time for the noise driven escape from this resting value to threshold; and third, the absolute refractory period.

The other dynamical regime is the *deterministic firing (suprathreshold) regime* for $v^* = \mu > v_T$. Here, the neuron fires at vanishing noisy driving in a strictly periodic fashion. Since the resting value is beyond the threshold, the voltage will always relax to this value and there is only relaxation time and absolute refractory period present in the system.

The dynamical behavior of the model can be characterized by several measures.

(1) The stationary spike rate characterizes the activity of the neuron regardless of randomness or periodicity of the spike train. The rate is given by the mean output of the
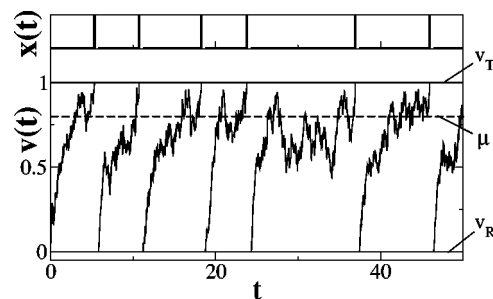

FIG. 1. Trajectory of the voltage variable $v(t)$ [evolving from Eq. (1)] and spike train for $\mu = 0.8$, $D = 0.015$, $v_T = 1$, $v_R = 0$, $\tau = 0.5$.

neuron and coincides with the inverse mean interspike interval ($\langle \cdot \rangle$ denotes the ensemble average)

$$r_0 = \langle x(t) \rangle = \frac{1}{\langle T \rangle}, \tag{4}$$

(for a derivation, see, for instance, Ref. [13]).

(2) The coefficient of variation, (CV) i.e., the relative standard deviation of the interspike interval, measures the uncertainty of the single interspike interval

$$R = \frac{\sqrt{\langle \Delta T^2 \rangle}}{\langle T \rangle}, \tag{5}$$

with $\langle \Delta T^2 \rangle = \langle (T - \langle T \rangle)^2 \rangle$ being the variance of interspike intervals. Poissonian spiking is associated with $R = 1$ whereas a strictly periodic spike train leads evidently to $R = 0$. In general, a low CV indicates a regular spike train, a high value indicates a large incoherence of spiking.

(3) The diffusion coefficient of the spike count determines how fast the variance of the spike count grows, hence, it is like the CV a measure of spike train incoherence. For a renewal process it can be also expressed by the moments of the interspike interval [14]

$$D_{\text{eff}} = \frac{1}{2} \lim_{t \to \infty} \frac{d}{dt} \langle n^2(t) - \langle n(t) \rangle^2 \rangle = \frac{1}{2} \frac{\langle \Delta T^2 \rangle}{\langle T \rangle^3}. \tag{6}$$

(4) The power spectrum of $\tilde{x}(t) = x(t) - \langle x(t) \rangle$ measures the periodic components of the spike train. It is related by a formula from renewal theory to the characteristic function of the interspike interval $\varrho(\omega)$ (i.e., the Fourier transform of the interspike interval density, see, e.g., Ref. [15])

$$S_{\tilde{x}}(\omega) = \int_{-\infty}^{\infty} d\tilde{\tau} \langle \tilde{x}(t) \tilde{x}(t + \tilde{\tau}) \rangle e^{i\omega\tilde{\tau}} = r_0 \frac{1 - |\varrho(\omega)|^2}{|1 - \varrho(\omega)|^2}. \tag{7}$$

Note that the spectrum at vanishing and infinite frequency is related to the diffusion coefficient of the spike count, coefficient of variation, and the spike rate, respectively, as follows:

$$\lim_{\omega \to 0} S(\omega) = 2D_{\text{eff}} = R^2 r_0, \; \lim_{\omega \to \infty} S(\omega) = r_0. \tag{8}$$

For the LIF model, all these functions can be calculated. The spike rate and coefficient of variation are known for a long time (see, e.g., Refs. [16,17] and references therein). In fact, the first three measures are given in terms of the first two moments of the sum of the first passage time from $v = v_R$ to $v = v_T$ [18] and the absolute refractory period. We have found that the original formulas involving up to four quadratures (see, e.g., Ref. [19]) can be written more compactly as

$$\langle T \rangle = \tau + \sqrt{\pi} \int_{(\mu - v_T)/\sqrt{2D}}^{(\mu - v_R)/\sqrt{2D}} dy\, e^{y^2} \text{erfc}(y), \tag{9}$$

$$\langle \Delta T^2 \rangle = 2\pi \int_{(\mu - v_T)/\sqrt{2D}}^{\infty} dy\, e^{y^2} [\text{erfc}(y)]^2$$

$$\times \int_{(\mu - v_T)/\sqrt{2D}}^{y} dz\, e^{z^2} \Theta\left(\frac{\mu - v_R}{\sqrt{2D}} - z \right), \tag{10}$$

where $\Theta(\cdot)$ denotes the Heaviside function. The integrals above have to be evaluated numerically.

For calculation of the power spectrum the characteristic function of the interspike interval, i.e., the Fourier transform of the interspike interval probability density is needed. This is given by $\rho(\omega) = \rho_{FP}(\omega) \rho_\tau(\omega)$, i.e., the product of the Fourier transforms of the first passage time distribution for the Ornstein-Uhlenbeck process and of the distribution for the deterministic absolute refractory period. The first function is known for decades [20] and reads in our notation

$$\rho_{FP}(\omega) = e^\delta \frac{\mathcal{D}_{i\omega}\left(\frac{\mu - v_R}{\sqrt{D}} \right)}{\mathcal{D}_{i\omega}\left(\frac{\mu - v_T}{\sqrt{D}} \right)}, \delta = \frac{v_R^2 - v_T^2 + 2\mu(v_T - v_R)}{4D}, \tag{11}$$

where $\mathcal{D}_a(z)$ denotes the parabolic cylinder function [21] that can be obtained by means of computer programs like MATHEMATICA or MAPLE. The characteristic function of the absolute refractory period is given by

$$\rho_\tau(\omega) = e^{i\omega\tau} \tag{12}$$

and, hence, the spectrum can be determined according to Eq. (7),

$$S_{\tilde{x}}(\omega) = r_0 \frac{\left| \mathcal{D}_{i\omega}\left(\frac{\mu - v_T}{\sqrt{D}} \right) \right|^2 - e^{2\delta} \left| \mathcal{D}_{i\omega}\left(\frac{\mu - v_R}{\sqrt{D}} \right) \right|^2}{\left| \mathcal{D}_{i\omega}\left(\frac{\mu - v_T}{\sqrt{D}} \right) - e^\delta e^{i\omega\tau} \mathcal{D}_{i\omega}\left(\frac{\mu - v_R}{\sqrt{D}} \right) \right|^2}, \tag{13}$$

an exact result that is, to our knowledge, new.

The quantities introduced can be also estimated by computer simulations. In order to verify our analytical results, we have used a simple Euler scheme with a time step between 10^{-3} and 10^{-5} (latter at high noise intensity) for the integration of Eq. (1). Up to 5×10^5 spikes were used to estimate the mean and variance of the interspike interval as well as the power spectrum of the spike train. The results of simulations were always in very good agreement with our analytical results as it should be.

It is well known that the effect of coherence resonance relies on the presence of at least two time scales with distinct noise dependences in the system [2]. In the LIF model these are the aforementioned relaxation and escape times. Even at vanishing absolute refractory period, the relaxation time may introduce a certain regularity in the spike train since at moderate noise intensity it can be larger than the activation time but still show only a small jitter.
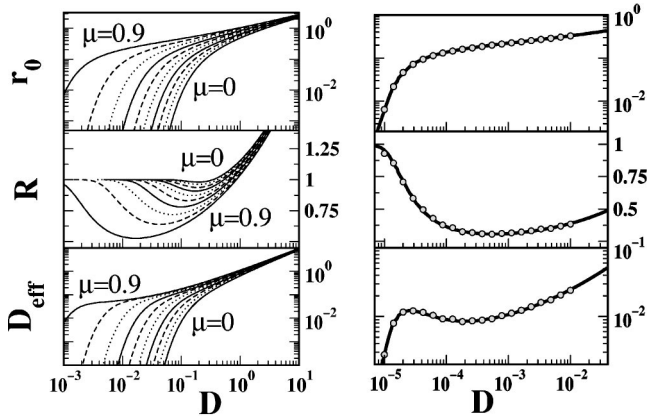
FIG. 2. Analytical results for rate, coefficient of variation, and diffusion coefficient of spike count vs noise intensity for $\tau=0$. Left: parameter μ is varied from 0 to 0.9 in steps of 0.1. Right: for $\mu=0.99$ compared to results (circles) from a numerical simulation of the model.

The ratio between relaxation and activation time scale (i.e., the ratio of the correponding mean passage times) can be monotonically changed by varying μ. An increase of the base current yields a longer relaxation from the reset point to resting voltage $v^*=\mu$ and decreases at the same time the distance from resting voltage to threshold and thus the escape time. Hence, increasing μ increases generally the coherence of spike train and—if μ remains subthreshold—leads to a more pronounced coherence resonance.

In Fig. 2 coherence resonance is demonstrated for the leaky integrate-and-fire model in the noise-activated firing regime ($\mu<1$). In order to verify that the effect is not due to the presence of a finite refractory period we set $\tau=0$. While the effect is only weakly present for small base currents ($\mu=0\ldots0.5$) we find a pronounced minimum in the coefficient of variation for larger but subthreshold values of μ ($\approx0.5\ldots0.9$). The diffusion coefficient of the spike count increases only monotonically. A new feature is observed if the base current is even further increased. At $\mu=0.99$ (Fig. 2, rhs) the coherence at optimal noise implies a minimum in the diffusion coefficient of the spike count that occurs at a slightly smaller value of D. This minimum is remarkable because the rate increases with noise intensity also in the range of decreasing diffusion.

The maximized coherence can also be seen in the power spectral density (Fig. 3). The neuron possesses a noise-induced eigenfrequency, which appears as a peak in the spectrum. This peak is most pronounced for an "optimal" noise. Note that spectra with a dip at low frequency and a peak at finite frequency have also been obtained from data of real neurons and nondynamical models of spike train generation in Ref. [22]. The resonance can be quantified by the degree of coherence as introduced in Ref. [12], i.e,

$$\beta=\frac{S(\omega_{\max})-r_0}{\Delta\omega/\omega_{\max}} \qquad (14)$$

where $\omega_{\max}$ is the frequency of the first peak and $\Delta\omega$ is the half-width of the respective peak over the high-frequency
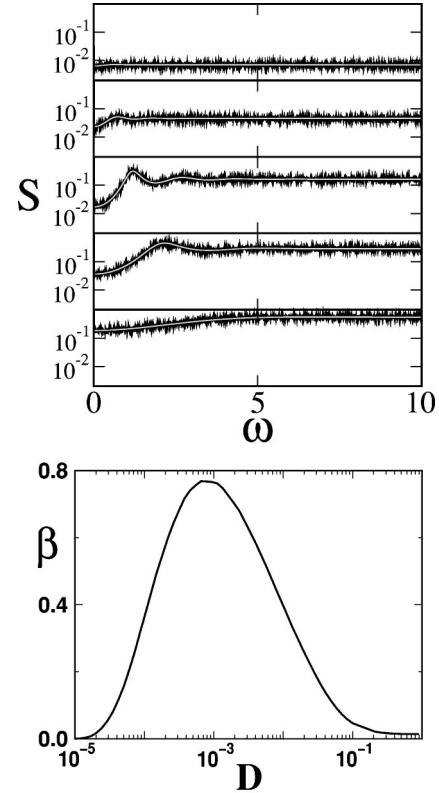

FIG. 3. Power spectra for different noise intensities (top) and the degree of coherence vs noise intensity (bottom) at $\mu=0.99$, $\tau=0$. From top to bottom: $D=10^{-5}$, 2×10^{-5}, 2×10^{-4}, 5×10^{-3}, 10^{-1}, theory (gray) according to Eq. (13) compared to simulations (black).

limit $[S(\omega\rightarrow\infty)=r_0]$. The function β that was numerically determined using Eq. (13) is shown in Fig. 3 (bottom) and reveals a maximum at roughly the same noise intensity as R and D_{eff}. Note that according to Eq. (8) the minimal values of R and D_{eff} correspond to the minimal values of $S(\omega=0)$ and $S(\omega=0)/S(\omega\rightarrow\infty)$, hence, all measures of CR can be described by different noise-dependent features of the power spectrum.

Up to this point we have not taken into account the absolute refractory period—the third time scale in the system. For a finite but small value $\tau=0.1$ (measured in units of the membrane time constant, which we have set to equal 1), the measures of CR do not change much for small to moderate noise intensity. However, the firing rate of the neuron is now restricted ($r_0<1/\tau$), i.e., in the somewhat trivial strong noise limit the neuron fires strictly periodically with a period that tends to the inverse of the refractory period. This again means that in both dynamical regimes, the coherence *can be minimized* (or *incoherence maximized*) for a finite value of the noise intensity. Consequently, the coefficient of variation as well as the diffusion coefficient of the spike count pass through *maxima* as functions of noise. This is necessarily the case in the deterministic firing regime where the neuron fires strictly periodically in either limits of vanishing and infinite noise intensity.

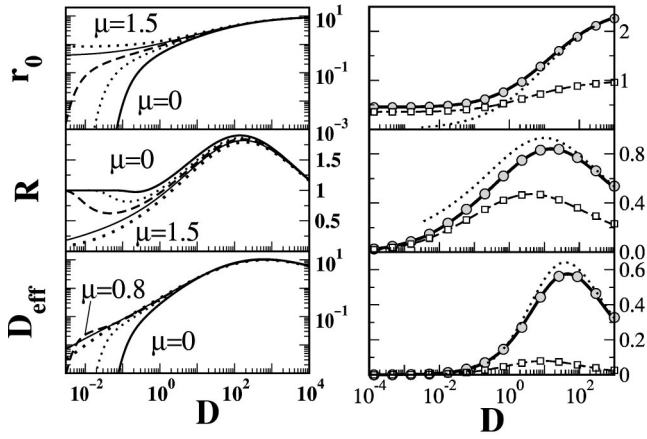If the refractory period is small ($\tau=0.1$ corresponds to

FIG. 4. Analytical results for rate, coefficient of variation, and diffusion coefficient of spike count vs noise intensity for finite τ. Left $\tau = 0.1$, μ is varied: 0 (solid), 0.5 (dotted), 0.8 (dashed), 1.1 (thin solid), 1.5 (thick dotted). Right, for $\mu = 1.2$, $\tau = 0.4$ (solid) and $\tau = 1$ (dashed) compared to numerical simulation results (circles and squares), dotted lines give the strong noise expressions according to Eqs. (15) for $\tau = 0.4$.

one-tenth of the membrane time constant), the incoherence is maximized at a rather large noise intensity (Fig. 4, lhs). For larger values of τ ($\tau = 0.4$ or 1) the maximum in the CV is shifted towards smaller values of D while the maximal CV is reduced by increasing τ (Fig. 4, rhs). These features can be also extracted from the large noise asymptotics of R and D_{eff}. Expanding the mean and variance of the interspike interval to first order in $1/\sqrt{D}$ yields ($v_R = 0, v_T = 1$)

$$r_0 \approx 1/[\tau + \sqrt{\pi}/\sqrt{2D}],$$

$$R \approx \sqrt{c_1} \frac{(2D)^{1/4}}{1 + \tau\sqrt{2D/\pi}}, \qquad (15)$$

$$D_{\text{eff}} \approx c_1 \frac{D/\sqrt{\pi}}{(1 + \tau\sqrt{2D/\pi})^3},$$

where c_1 is a constant ($c_1 \approx 0.782$). By the latter two expressions, it is possible to estimate the locations of maxima of $R(D)$ and $D_{\text{eff}}(D)$, respectively,

$$D_{\text{Rmax}} \approx \pi/(2\tau^2)$$

$$D_{D_{\text{eff}}\text{max}} \approx 2\pi/\tau^2 = 4D_{\text{Rmax}}. \qquad (16)$$

From this, the following conclusions can be drawn which are also confirmed by comparison with the exact results: (i) locations of maxima are independent of base current (cf. Fig. 4, lhs) (ii) maxima shift towards smaller D for increasing τ (cf. Fig. 4, lhs and rhs), (iii) D_{eff} attains its maximum at a larger noise intensity than the CV does, and (iv) CV is maximized if the rate is half of its maximal value [$r_0(D_{\text{Rmax}}) \approx 1/(2\tau)$]. The approximations (15) and (16) better describe
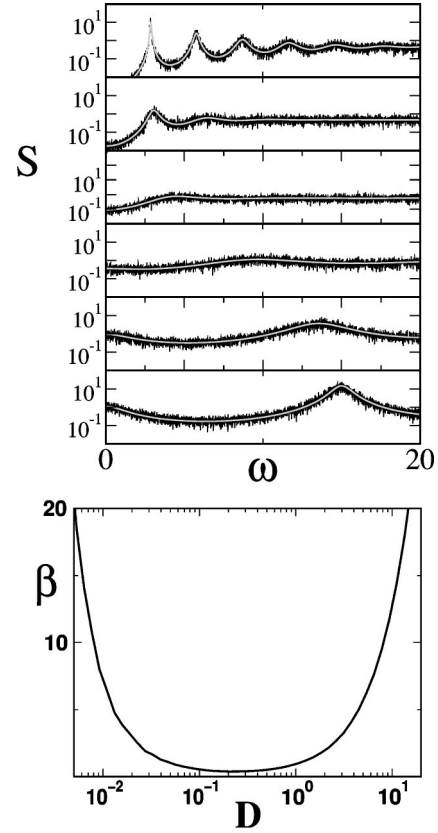

FIG. 5. Power spectra (top) in the deterministic firing regime for different noise intensities and spectral coherence (bottom) as a function of noise intensity at $\mu = 1.2$, $\tau = 0.4$. From top to bottom: $D = 10^{-3}, 10^{-2}, 10^{-1}, 10^0, 10^1, 10^2$, theory (gray) according to Eq. (13) compared to simulations (black).

the features of maxima the smaller τ is. For comparison, we show in Fig. 4 (rhs, dotted line) the approximations according to Eq. (15) for $\tau = 0.4$.

The incoherence maximization becomes apparent also in the power spectra. In the deterministic firing regime and for $\tau = 0.4$, for instance (these are reasonable parameters for many systems [23]), the spectrum at weak noise exhibits large peaks around the deterministic eigenfrequency and its higher harmonics (Fig. 5, upper panels). For growing noise the spectrum becomes "featureless" (Fig. 5, mid panels) whereas at large noise intensity again a peak appears due to the finite absolute refractory period (Fig. 5, lower panels). Consequently, the degree of coherence goes through a minimum as a function of noise. Remarkably, the spectral incoherence is maximized (β is minimized) at lower noise than the CV and the diffusion coefficient of the spike count. For example, for $\tau = 0.4$ the CV attains its maximum for $D \approx 16$, the degree of spectral coherence is minimized at $D \approx 0.2$. In between these values an increase in noise intensity leads not only to growing variability but also to an increase in the periodic component of the spike train. This is due to two competing effects: growing noise makes large excursions of the voltage variable towards negative values possible, thus increasing the variability of the interspike interval; it leads, however, also to sequences of subsequent short pas-
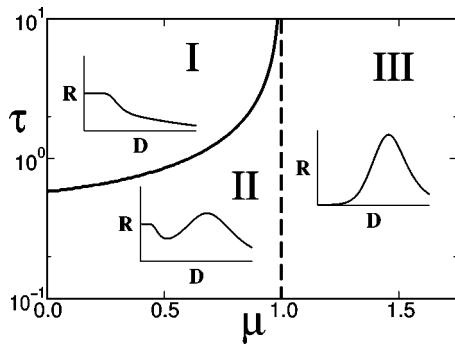
FIG. 6. Lines in parameter plane (τ,μ) separating regions where the R is a monotonic function of D (region I), a function with minimum and maximum (II), or a function with just one maximum (III). The insets show the corresponding shapes of the R vs D curves.
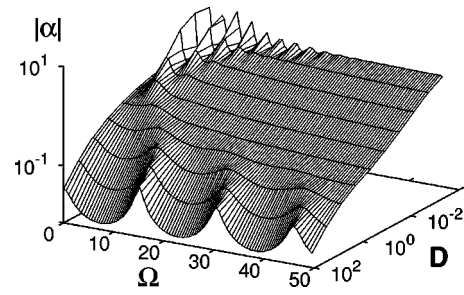

FIG. 7. Response amplitude with respect to an additive periodic signal as a function of noise intensity and driving frequency for $\mu = 1.2$ and $\tau = 0.4$.

sages from the reset to the threshold level, thereby enlarging the spectral coherence that measures the periodicity. With respect to the transmission of time dependent signals, the minimum in spectral coherence is certainly more important (see below) than the maximum in the CV vs noise strength. This is remarkable since the noise intensity of maximized spectral incoherence is biologically more plausible than the values obtained for maximal CV.

The effect found may be also observed in the noise-activated firing regime if the absolute refractory period is sufficiently small. The respective value of τ will depend on the base current. This is illustrated for the coefficient of variation in Fig. 6. For parameter values to the left of the dashed line and below the solid line (region II), the CV shows a minimum (coherence resonance) and a maximum (incoherence maximization). For values above the solid line (region I), CV drops monotonically from 1 (Poisson limit) to zero. As mentioned above, for base currents larger than 1 (region III), the CV necessarily has to go through a maximum, however, there is no coherence resonance (i.e., minimum vs D) in this case. We note that the biologically relevant region is below the line $\tau=1$, hence, within the regions (II and III) where the CV has at least a maximum.

One may relate certain transmission features of neuron models to our findings. The driving used in our study, i.e., a constant base current and noise of a constant intensity reflects the influence of neuronal synaptic background rather than a realistic signal added to this background. How do the effects of coherence resonance and incoherence maximization influence the transmission of such additional (for instance, periodic) stimuli?

For periodically driven LIF neurons (studied, e.g., in Refs. [24–30]), a strong resonance in the response can be expected if the power spectrum exhibits one or several strong eigenfrequencies [26,27]. More generally, a broadband signal (i.e., a superposition of periodic signals with given frequency distribution) is distorted, i.e., only a certain frequency band is filtered—a property that can be considered as a simple form of signal processing. This filtering can be realized either by neurons operating in the deterministic firing regime

or in the noise-activated firing regime *at a suitable noise level* [26,28]. The latter is a consequence of coherence resonance [10,29].

In contrast, a rather uniform transmission is expected if the power spectrum is broad (i.e. featureless). In other words, a periodic signal will be transmitted largely irrespective of its frequency and a broadband signal will be reproduced without distortion [30]. A noise level that maximizes the incoherence of spike train is thus associated with a minimized distorted signal transmission.

To illustrate the latter property we use the results from Ref. [27] where the transmission of periodic additive and noise coded signals were studied. For a weak periodic modulation of base current, i.e., $\mu \rightarrow \mu + \varepsilon \cos(\omega t)$ the asymptotic firing rate of a LIF neuron will be time dependent according to $r(t)=r_0+\varepsilon|\alpha|\cos(\Omega t+\phi)$ where α is the response amplitude and ϕ is the phase lag. The response amplitude reads [27]

$$\alpha = \frac{r_0 i\Omega/\sqrt{D}}{i\Omega - 1} \frac{\mathcal{D}_{i\Omega-1}\left(\frac{\mu-v_T}{\sqrt{D}}\right) - e^{\delta}\mathcal{D}_{i\Omega-1}\left(\frac{\mu-v_R}{\sqrt{D}}\right)}{\mathcal{D}_{i\Omega}\left(\frac{\mu-v_T}{\sqrt{D}}\right) - e^{\delta}e^{i\Omega\tau}\mathcal{D}_{i\Omega}\left(\frac{\mu-v_R}{\sqrt{D}}\right)}.$$

(17)

A plot of the response amplitude vs driving frequency and noise intensity for suprathreshold base current and finite absolute refractory period (Fig. 7) reveals strong resonances for small and large noise intensities occurring at the deterministic eigenfrequency and at the inverse of the refractory period multiplied by 2π, respectively. At moderate noise intensity where the incoherence maximization in the absence of periodic modulation was observed (corresponding to the minimum in spectral coherence β), however, the response does not depend crucially on driving frequency; of course, this has come at the cost of a significantly reduced response amplitude compared to that in the low noise case. For the response to a noise coded signal one finds a similar behavior (not shown).

In conclusion, we have shown that tuning the input's

noise level may either minimize or maximize the coherence of the spike train generated by a simple model neuron. Hence, noise can confer either a pronounced or a flat band-pass characteristic to a neuronal system, and thus signifi-

cantly change the transmission of temporally varying (non-static) signals.

[1] H. Gang, T. Ditzinger, C.Z. Ning, and H. Haken, Phys. Rev. Lett. **71**, 807 (1993).

[2] A. Pikovsky and J. Kurths, Phys. Rev. Lett. **78**, 775 (1997).

[3] A. Longtin, Phys. Rev. E **55**, 868 (1997).

[4] A. Neiman, P.I. Saparin, and L. Stone, Phys. Rev. E **56**, 270 (1997).

[5] L. I and J.-M. Liu, Phys. Rev. Lett. **74**, 3161 (1995).

[6] D.E. Postnov, S.K. Han, T.G. Yim, and O.V. Sosnovtseva, Phys. Rev. E **59**, R3791 (1999).

[7] G. Giacomelli, M. Giudici, S. Balle, and J.R. Tredicce, Phys. Rev. Lett. **84**, 3298 (2000).

[8] D. Wilkowski, J. Ringot, D. Hennequin, and J.C. Garreau, Phys. Rev. Lett. **85**, 1839 (2000).

[9] B. Lindner and L. Schimansky-Geier, Phys. Rev. E **60**, 7270 (1999).

[10] B. Lindner and L. Schimansky-Geier, Phys. Rev. E **61**, 6103 (2000).

[11] Y. Yu, W. Wang, J. Wang, and F. Liu, Phys. Rev. E **63**, 021907 (2001).

[12] K. Pakdaman, S. Tanabe, and T. Shimokawa, Neural Networks **14**, 895 (2001).

[13] F. Rieke, D. Warland, R. de Ruyter van Steveninck, and W. Bialek. *Spikes: Exploring the Neural Code* (MIT Press, Cambridge, MA, 1996).

[14] D. R. Cox, *Renewal Theory* (Methuen, London, 1962).

[15] R. L. Stratonovich, *Topics in the Theory of Random Noise* (Gordon and Breach, New York, 1967).

[16] L. M. Ricciardi *Diffusion Processes and Related Topics on Biology* (Springer-Verlag, Berlin, 1977).

[17] H. C. Tuckwell *Introduction to Theoretical Neurobiology* (Cambridge University Press, Cambridge, 1988).

[18] L. Pontryagin, A. Andronov, and A. Witt, Zh. Eksp. Teor. Fiz. **3**, 172 (1933); Reprinted in *Noise in Nonlinear Dynamics*, edited by F. Moss and P. V. E. McClintock (Cambridge University Press, Cambridge, 1989), Vol. 1, p. 329.

[19] C. W. Gardiner, *Handbook of Stochastic Methods* (Springer-Verlag, Berlin, 1985).

[20] D.A. Darling and A.J.F. Siegert, Ann. Math. Stat. **24**, 624 (1953).

[21] M. Abramowitz and I. A. Stegun *Handbook of Mathematical Functions* (Dover, New York, 1970).

[22] J. Franklin and W. Bair, SIAM (Soc. Ind. Appl. Math.) J. Appl. Math. **55**, 1074 (1995).

[23] C. Koch, *Biophysics of Computation—Information Processing in Single Neurons* (Oxford University Press, New York, 1999).

[24] A. Bulsara, T.C. Elston, Ch.R. Doering, S.B. Lowen, and K. Lindenberg, Phys. Rev. E **53**, 3958 (1996).

[25] T. Shimokawa, K. Pakdaman, and S. Sato, Phys. Rev. E **59**, 3427 (1999).

[26] H.E. Plesser and T. Geisel, Phys. Rev. E **59**, 7008 (1999).

[27] B. Lindner and L. Schimansky-Geier, Phys. Rev. Lett. **86**, 2934 (2001).

[28] H.E. Plesser and T. Geisel, Neurocomputing **26/27**, 229 (1999).

[29] B. Lindner *Coherence and Stochastic Resonance in Nonlinear Dynamical Systems* (Logos-Verlag, Berlin 2002).

[30] B.W. Knight, J. Gen. Physiol. **59**, 734 (1972).